Support information for:

Boosted Li^+ Transference Number Enabled via Interfacial Engineering for Dendrite-Free Lithium Metal Anodes

*Ting Zeng, Yu Yan, Miao He, Ruixin Zheng, Dayue Du, Longfei Ren, Bo Zhou and Chaozhu Shu**

College of Materials and Chemistry & Chemical Engineering, Chengdu University of Technology, 1#, Dongsanlu, Erxianqiao, Chengdu 610059, Sichuan, P. R. China

**E-mail: czshu@imr.ac.cn; shuchaozhu13@cdut.edu.cn (Chaozhu Shu).*

1. Experimental section

Synthesis of ZIF-67 Nanoparticles: ZIF-67 nanoparticles are synthesized according to a reported solution-precipitation method. 1.642 g 2-methylimidazole and 1.455 g cobalt nitrate hexahydrate are dissolved in 80 mL methanol. The precipitate of the solution is washed with CH_3OH for three times and dried in 60 °C overnight, and then dried under vacuum at 200 °C.

Fabrication of Artificial Protective Layer: Firstly, 0.45 g ZIF-67 powders and 0.05 g PVDF are dispersed in NMP solvent. After that, the dispersion is doctor bladed on Cu foil followed by drying at 60 °C overnight.

Material characterization: X-ray diffraction (XRD) patterns are recorded by using a D/MAX-IIIC (Japan) with Cu Kα radiation with scanning range from 5° to 80°. Thermalgravimetric analysis (TGA) profiles are obtained on a TA-Q500 thermogravimetric analyzer with a heating rate of 5 °C min^{-1} in N_2 atmosphere. Nitrogen adsorption–desorption measurements at 77 K are performed on an Autosorb-iQ2-MP (Quantachrome Instruments) surface area analyzer. Scanning electron microscopy (SEM) is recorded by using a JSM-6700F. X-ray photo electron spectra (XPS) are conducted by using an ESZALB 250XL spectrometer with a Al K Alpha X-ray source.

Electrochemical measurements: ZIF-67-Cu symmetric cells and half cells were assembled in an argon-filled glove box (H_2O< 0.1 ppm, O_2< 0.1 ppm) with 1 M lithiumbis(trifluoromethanesulfonyl)imide in 1,3-dioxolane (DOL)/1,2-dimethoxyethane (DME) (1:1 w/w) as electrolyte and Celgard 2400 as separator. Each

cell contains ~30 μL electrolyte. For the control samples, bare Cu and pure Li were employed to replace the ZIF-67-Cu, making symmetric cells and half cells with the other conditions to be the same. A certain amount of Li was deposited onto the current collectors and then charged to 1.0 V (vs Li/Li^+) to strip the Li for each cycle, during which the Coulombic efficiency were calculated. Nucleation overpotential was obtained from the galvanostatic discharge curves at a current density of 0.5 mA cm^{-2}. The nucleation overpotential is defined as the voltage difference between the sharp tip voltage and the following stable mass transfer-controlled overpotential. To evaluate the cycling stability, 5 mA h cm^{-2} Li was first pre-deposited on the current collectors at 0.5 mA cm^{-2}. After that, 0.5 mA h cm^{-2} Li was stripped from the deposited lithium and then plated to ZIF-67-Cu@Li, Cu@Li electrodes at 0.5 mA cm^{-2}. Li-O_2 batteries were also assembled in the argon-filled glove box by employing ZIF-67-Cu@Li as anode and Super P as cathode, glass fiber (Whatman, GF/D) as the separator, 1 M LiTFSI in TEGDME solution as electrolyte. The electrochemical impedance spectroscopy (EIS) test was carried out on electrochemical workstation (Metrohm Autolab, PGSTAT 302 N) at open circuit voltage with a voltage amplitude of 10 mV at a frequency range of 0.01-100 kHZ. Galvanostatic discharge/charge measurements were conducted on a Wuhan LAND battery testing system (CT2001A). The specific capacities and current densities were normalized based on the total mass of the material and binder.

2. Supporting Results and Figures

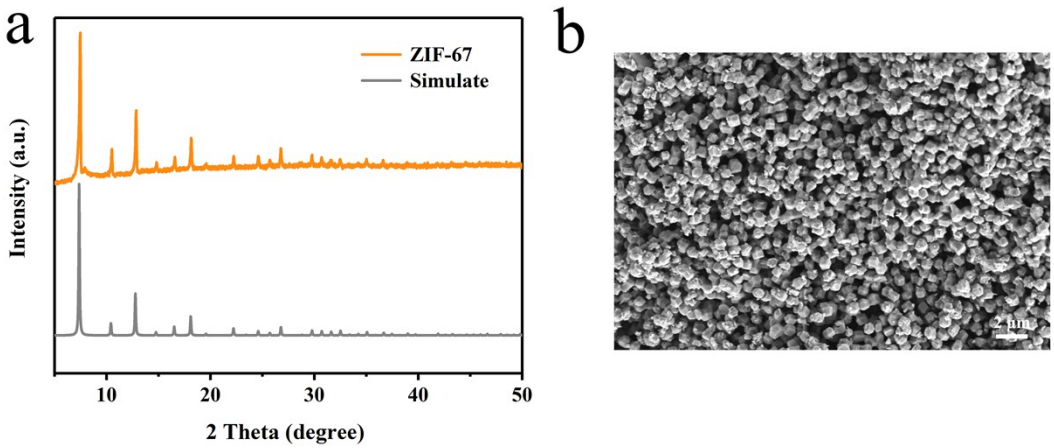

Figure S1. (a) XRD patterns of ZIF-67 and the simulated result. (b) SEM image of ZIF-67 nanoparticles.

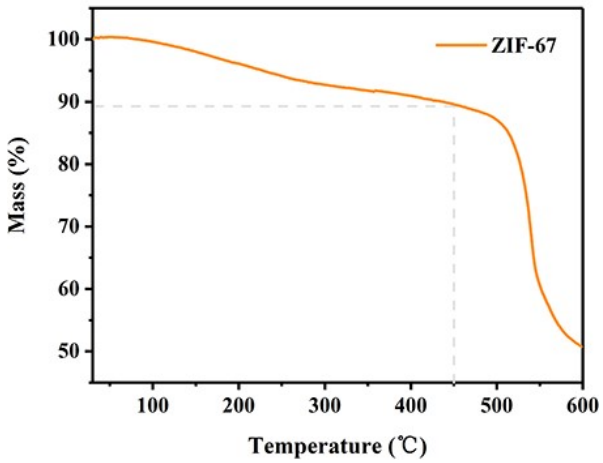

Figure S2. TGA curves of ZIF-67.

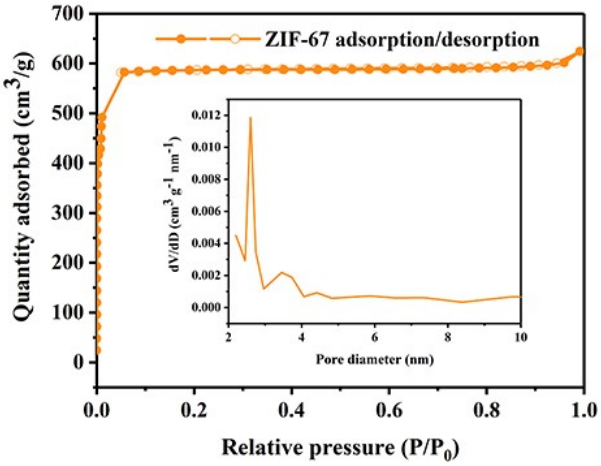

Figure S3. N_2 adsorption/desorption isotherm and pore size distribution of ZIF-67.

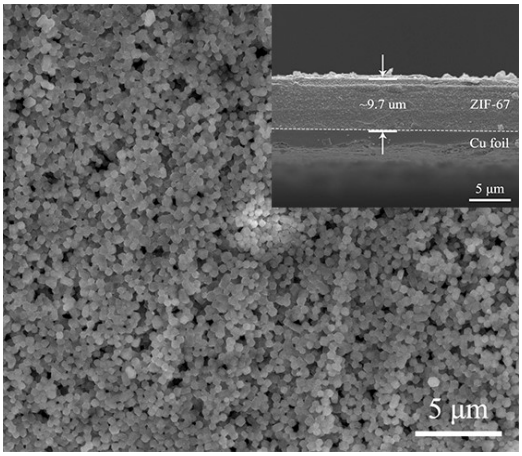

Figure S4. Top-view and cross-sectional SEM image (inset) of ZIF-67 layer.

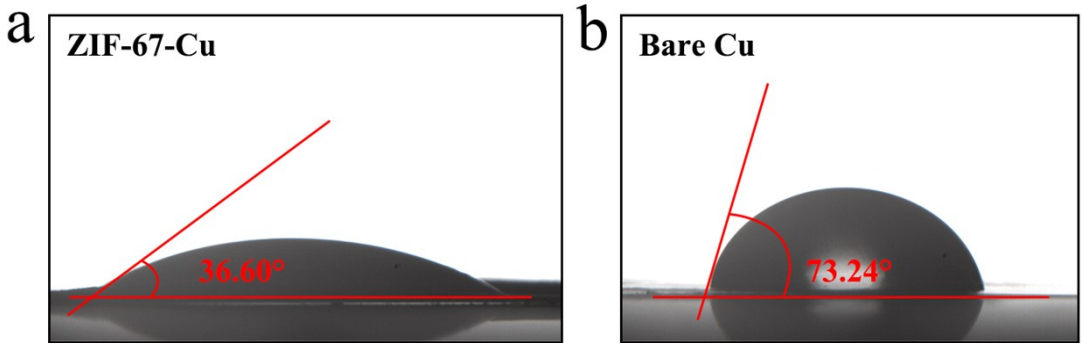

Figure S5. The contact angles between liquid electrolyte and (a) ZIF-67-Cu and (b) bare Cu electrode.

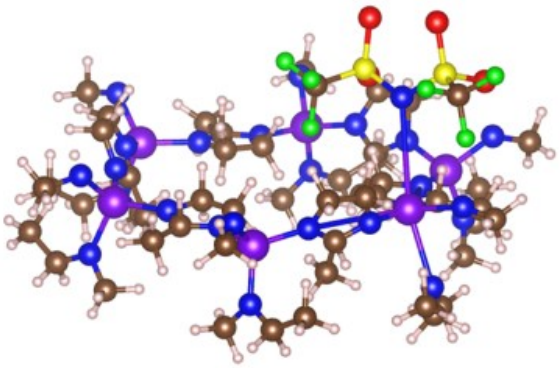

Figure S6. Density function theory (DFT) calculations of $TFSI^-$ ions adsorption configurations on unsaturated coordination metal sites of ZIF-67.

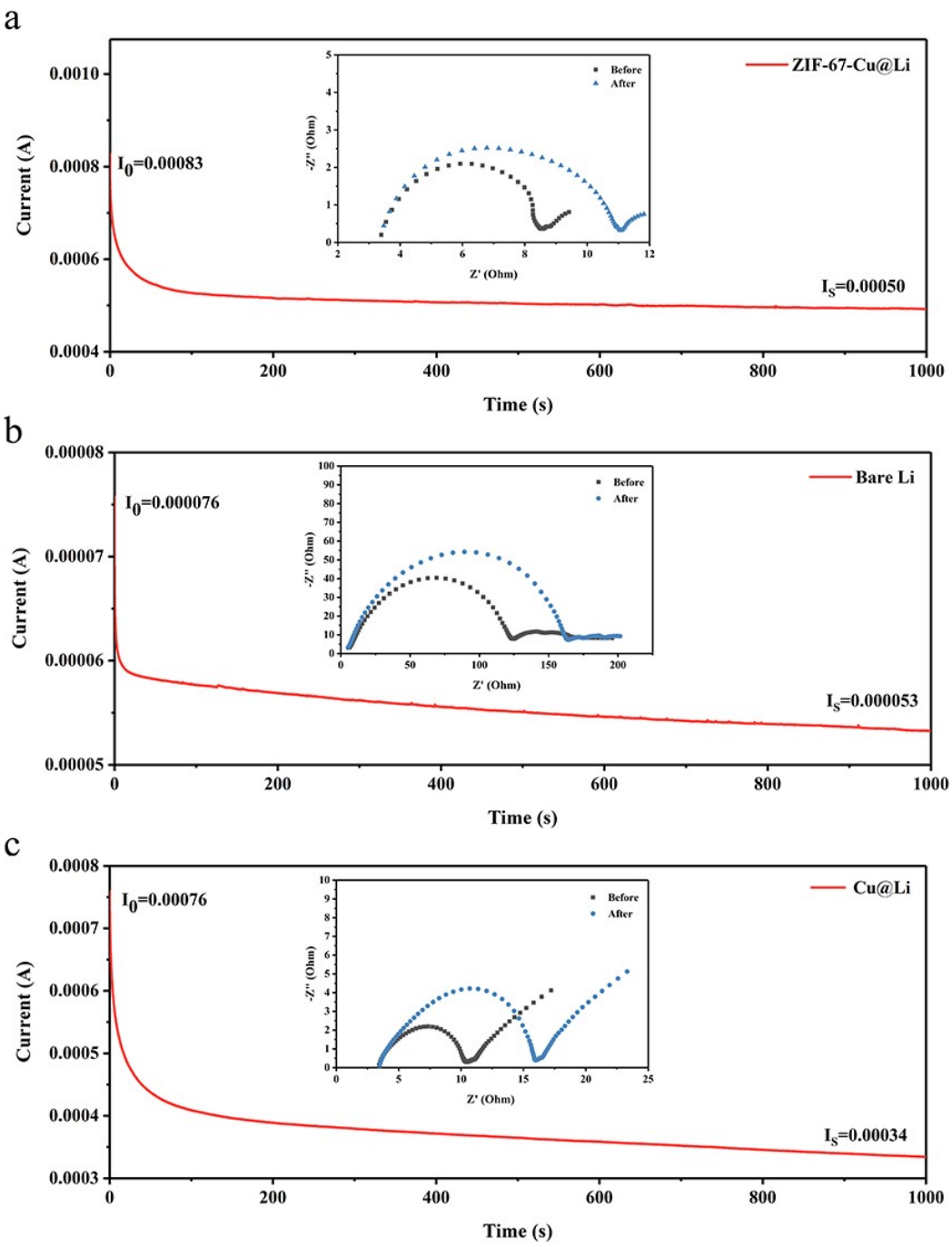

Figure S7. Chronoamperogram of (a) ZIF-67-Cu@Li, (b) bare Li and (c) Cu@Li symmetric cells with an applied voltage of 10 mV, respectively, I_0 and I_s indicate the initial current and the steady-state current. The inset is Nyquist plot of different symmetric cells before/after polarization, showing the initial and steady-state internal resistance.

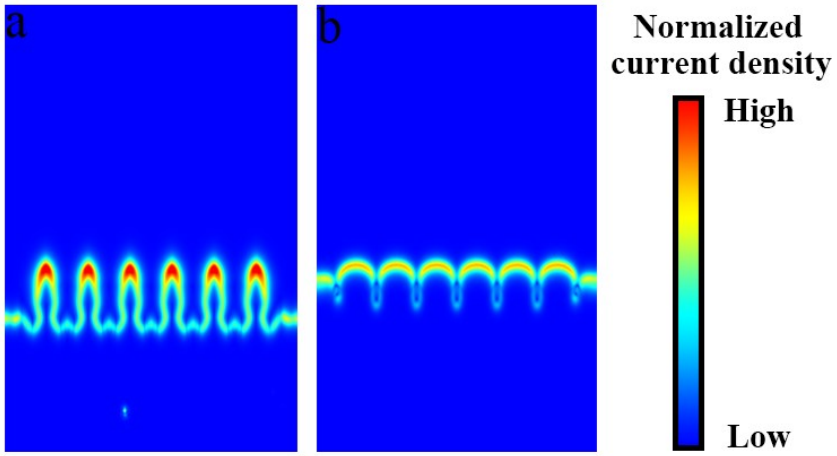

Figure S8. The simulated local current density distribution on (a) Cu@Li electrode and (b) ZIF-67-Cu@Li electrode at 1800s.

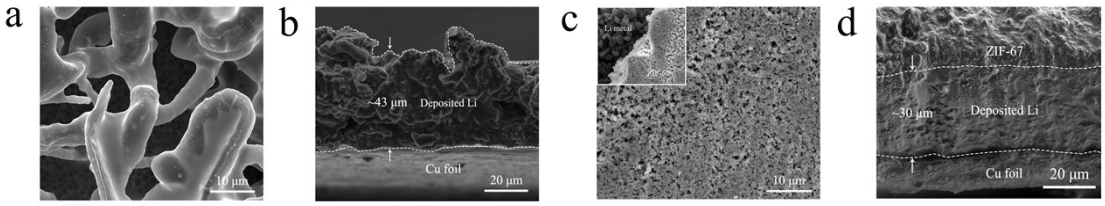

Figure S9. (a, c) Top-view and (b, d) cross-sectional SEM images of (a, b) Cu@Li and (c, d) ZIF-67-Cu@Li electrodes after plating 5 mAh cm^{-2} Li.

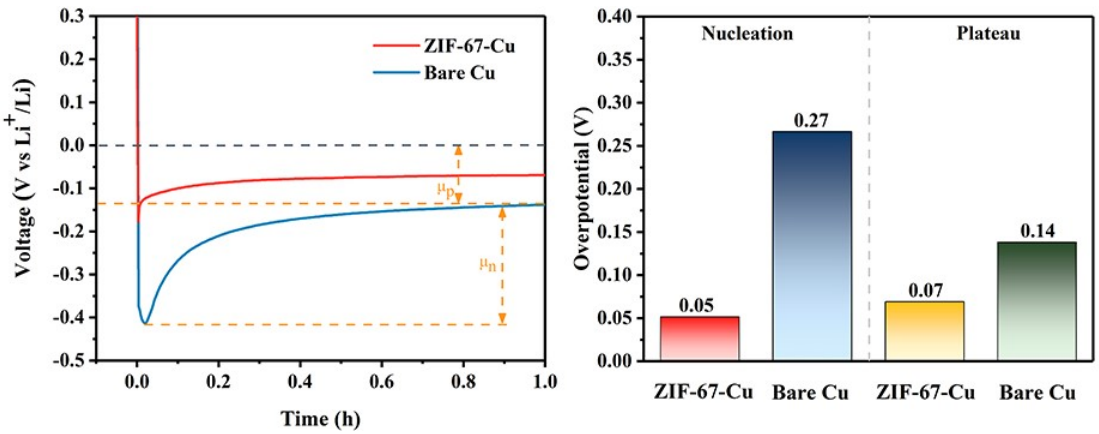

Figure S10. Voltage profiles of galvanostatic Li deposition on bare Cu and ZIF-67-Cu electrodes at a fixed current density of 0.5 mA cm^{-2} and the comparison of overpotentials at the nucleation and plateau regions.

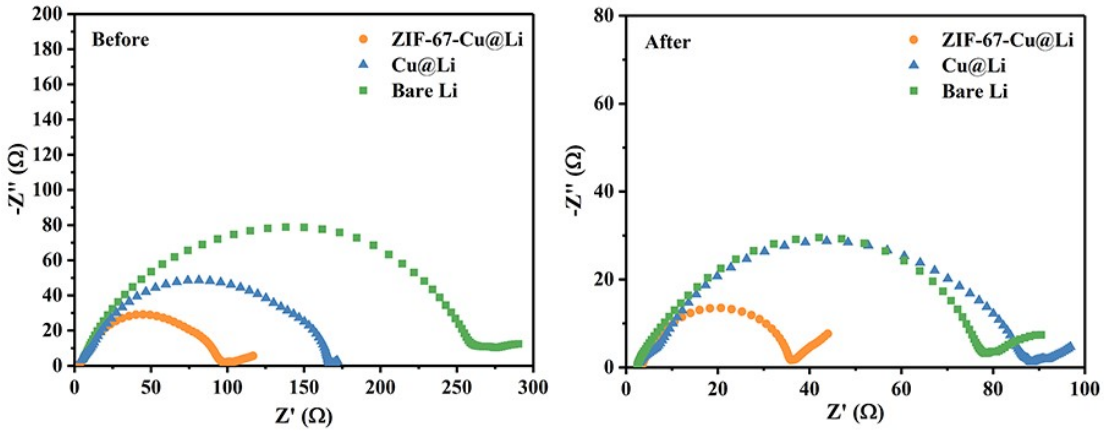

Figure S11. Electrochemical impedance spectroscopy curves of different symmetric cells before and after 100 cycles.

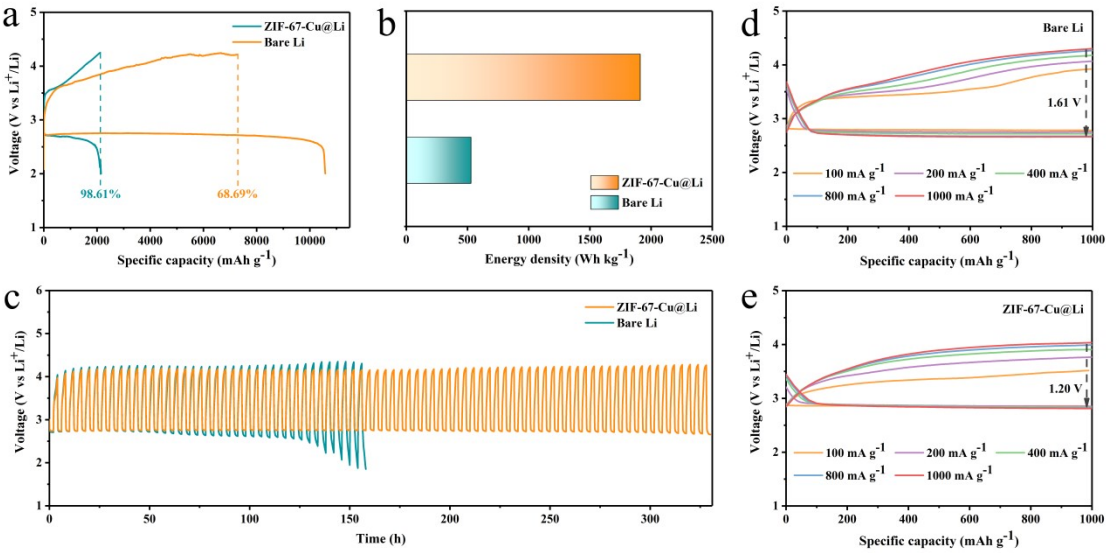

Figure S12. (a) The first discharge-charge curves of LOBs at a current density of 500 mA g-1 and (b) the corresponding energy density profile. (c) The cycle performance of both electrodes with a cut-off capacity of 1000 mAh g-1 at a current density of 500 mA g-1. The rate performance of the LOBs based on (d) bare Li and (e) ZIF-67-Cu@Li electrodes with a limited capacity of 1000 mAh g-1 at different current densities (100, 200, 400, 800 and 1000 mA g-1).

Supplementary video 1.mp4

Supplementary video 1 for Li deposition on bare Cu electrode.

Supplementary video 2.mp4

Supplementary video 2 for Li deposition on ZIF-67-Cu electrode.